Elastic properties of $Mg_xTi_{1-x}B_2(0 \leqslant x \leqslant 1)$ studied by first-principles calculations

David Groh,[1] William J. Slough,[1] Ravindra Pandey,[1,*] Shashi P. Karna,[2] and Dattatraya Dandekar[2,†]
[1]*Department of Physics, Michigan Technological University, Houghton, Michigan 49931, USA*
[2]*US Army Research Laboratory, Weapons and Materials Research Directorate, AMSRD-ARL-WM, Aberdeen Proving Ground, Maryland 21005, USA*
(Received 27 October 2010; revised manuscript received 25 January 2011; published 15 March 2011)

The elastic properties, including elastic constants, bulk, and shear moduli, and anisotropic index of hexagonal $Mg_xTi_{1-x}B_2$ ($0 \leqslant x \leqslant 1$) are obtained using a *first-principles* density-functional-theory method. A difference in chemical bonding occurs between Ti-rich and Mg-rich diborides, leading to significantly different elastic properties: a small elastic anisotropy with relatively large bulk and shear moduli for Ti-rich diborides with $x < 0.25$, and a large elastic anisotropy and relatively small bulk and shear moduli for Mg-rich diborides with $x > 0.25$. The calculated results reveal a dominant role of the interplanar metal-metal bonds in predicting the extent of shear elastic anisotropy in $Mg_xTi_{1-x}B_2$ ($0 \leqslant x \leqslant 1$).

DOI: 10.1103/PhysRevB.83.115122 PACS number(s): 71.20.Ps, 62.20.de

I. INTRODUCTION

Titanium diboride, TiB_2, is well known to be an ultrahigh-strength, highly ductile, and highly deformable material.[1] The physical and chemical properties of TiB_2 have been extensively studied by experimental[2–24] and theoretical methods.[25–34] Due to its high hardness, extreme melting point, and chemical inertness, TiB_2 is a candidate for a number of applications. Specifically, it is found to have large shear strength under high pressure[23] with a shear modulus value of 265 GPa.[24] The combination of high hardness and shear strength make it attractive for ballistic armor, but its relatively high density (4.50 gm/cm^3) (Ref. 2) makes it less attractive for this purpose than some other ceramics. One can consider a combination of magnesium (Mg) and TiB_2 as potentially bringing optimal materials characteristics in terms of its mechanical properties while at the same time making the resulting material system much lighter. Isomorphic MgB_2 is a light-weight material with a density of (2.66 gm/cm^3), but lacks shear strength compared to TiB_2. In the present study, we consider $Mg_xTi_{1-x}B_2$ ($0 \leqslant x \leqslant 1$), investigating its elastic properties using a *first-principles* density-functional theory (DFT) method. Specifically we calculate the variation of the structural and elastic properties of $Mg_xTi_{1-x}B_2$ with the dopant (Mg) concentration in the host (TiB_2) lattice. The composition of the ordered mixed system was chosen in such a way that the doping of Mg atoms maintained the hexagonal symmetry of the host TiB_2 requiring relatively modest computational resources for calculations. It is expected that such a fundamental understanding of the elastic properties of $Mg_xTi_{1-x}B_2$ will aid in determining its stability and shear strength for use as a lightweight impact-resistant material. It is also noted that there have been experimental efforts to incorporate Ti in MgB_2—a bulk superconductor—to improve its mechanical and superconducting properties.[35–37]

II. COMPUTATIONAL METHOD

A. Modeling of structure

Quantum-mechanical calculations based on DFT were performed using the CRYSTAL09 program.[38] A linear combination of Gaussian-type orbitals (GTO) is used to construct a localized atomic basis from which Bloch functions are constructed by a further linear combination with phase factors. The exchange and correlation effects were treated with the B3LYP functional form (i.e., Becke's three-parameter hybrid exchange functional[39] and the Lee, Yang, and Parr correlation functional[40]), which has been found to yield band gaps consistent with measured values for semiconducting and ionic materials.[41–47]

All-electron basis sets employed in the present study are the split-valence GTO basis sets consisting of three *s*- and two *p*-type shells for B (i.e., a 6-21G set), five *s*-, four *p*-, and one *d*-type shell for Ti (i.e., an 8-6411G set), and four *s*- and three *p*-type shells (i.e., an 8-511G set) for Mg.[31,48] The chosen level of basis sets has been demonstrated to be very good in providing accurate and reliable predictions of structural properties for a wide variety of materials, including Si, BN, GaN, GeC, PbF_2, Ga_2O_3, and boron.[41–47] Several higher levels of basis sets with polarization were also studied for boron yielding very similar structural properties for $Mg_4Ti_4B_{16}$ including lattice and elastic constants.[49] The integral overlap tolerances were 10^{-7} Hy and energy tolerance was 10^{-6} Hy in the iterative solution of the Kohn-Sham equations. The Brillouin zone was sampled with a $12 \times 12 \times 12$ Monkhorst grid for integrations in reciprocal space.

To calculate the structural and elastic properties of $Mg_xTi_{1-x}B_2$, we began with a supercell of Ti_8B_{16} representing the host, TiB_2. The cases of $x = 0$, 0.125, 0.25, 0.5. 0.75, and 1 can then be represented by Ti_8B_{16}, $Mg_1Ti_7B_{16}$, $Mg_2Ti_6B_{16}$, $Mg_4Ti_4B_{16}$, $Mg_6Ti_2B_{16}$, Mg_7TiB_{16}, and Mg_8B_{16}, respectively. Considering the fact that both TiB_2 and MgB_2 crystallize in the hexagonal AlB_2 structures, $Mg_xTi_{1-x}B_2$ ($0 \leqslant x \leqslant 1$) are assumed to be in the AlB_2-type structures (Fig. 1) in the present study. We emphasize that the reliability and accuracy of the chosen computational model was successfully tested on the well-studied TiB_2 system, closely reproducing its observed structural properties, as we discuss in the following section.

B. Calculation of elastic constants

The calculated variation of the total energy with the strain applied to induce deformation in the lattice is used to

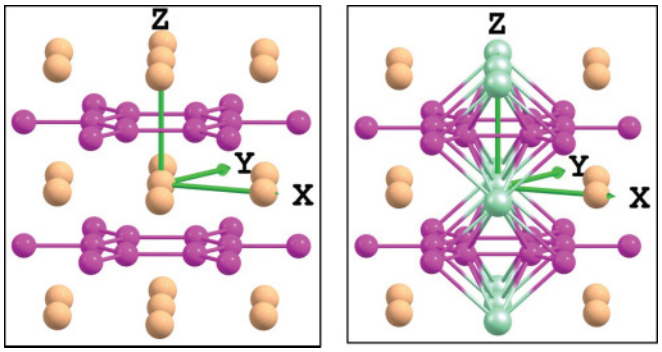

FIG. 1. (Color online) (Left) Ti_8B_{16} and (right) $Mg_4Ti_4B_{16}$ layered structure. Boron atoms are in purple, Ti atoms are in orange, and Mg atoms are in green.

determine the elastic properties of $Mg_xTi_{1-x}B_2$. For example, the second-order elastic constants, $C_{\alpha\beta}$, are obtained using variations (derivatives) of the equilibrium energy with respect to applied strains via the relation

$$C_{\alpha\beta} = \frac{1}{V}\frac{\partial^2 E}{\partial\varepsilon_\alpha \partial\varepsilon_\beta}, \quad (1)$$

where Voigt's notation is employed ($\alpha,\beta = 1,2,\ldots,6$), the ε are applied strains, and the variations are evaluated in the neighborhood of the minimum of the calculated energy for the crystal, E.[50]

In the equilibrium configuration of a given system, allowed deformations of the system are determined from the analysis of its space group, and these are used to generate a strain matrix, ε. Several numerical routines are employed to determine the change in energy of the crystal as a function of strain, which then yields the second-order elastic constants, $C_{\alpha\beta}$. Note that the atomic coordinates were fully optimized in these calculations.

III. RESULTS AND DISCUSSION

A. Structural properties

TiB_2 crystallizes in a hexagonal AlB_2 structure at ambient conditions with the space group of 191 (i.e., $P6/mmm$). The boron atoms are arrayed in graphene-type layers. Each layer of boron atoms is separated by a hexagonal layer of Ti atoms. Each atom in the Ti-layer lies above and below the center of an open hexagonal space in the graphene-type boron layer (Fig. 1). Twelve equidistant boron atoms are near neighbors for each Ti atom, whereas the near neighbors of each boron atom are three boron atoms at a short distance and six titanium atoms at a longer distance.[24] The experimental values of the lattice parameters a and c are 3.028 and 3.228 Å (Ref. 51) [or 3.0236 and 3.2204 Å (Ref. 2)], respectively.

The calculated structural properties of TiB_2 (or Ti_8B_{16}) at the B3LYP-DFT level of theory are in excellent agreement with the corresponding experimental values. For example, the calculated lattice parameters a and c are 3.0238 and 3.2254 Å, respectively, giving a unit-cell volume of 25.54 Å^3. The experimental value for the unit-cell volume is 25.5 Å^3, whereas previously reported first-principles calculations find the unit-cell volume of TiB_2 to be 25.1–25.7 Å^3.[26,28,31] A recent ultrasoft pseudopotential-generalized gradient approximation to DFT calculation reported the lattice constants a and c to be 3.0315 and 3.238 Å, respectively.[34]

Table I collects the optimized lattice parameters, unit-cell volume, density, and cohesive energy associated with the equilibrium configurations of $Mg_xTi_{1-x}B_2$ ($0 \leqslant x \leqslant 1$) obtained at the B3LYP-DFT level of theory. A gradual increase in the lattice parameters together with the equilibrium volume and density is predicted as the concentration of Mg increases in the TiB_2 lattice except in the case of a for $Mg_1Ti_7B_{16}$, which contracts slightly (≈0.2%) relative to that of the host Ti_8B_{16}. The variation of lattice parameters versus the concentration of Mg is shown in Fig. 2. In going from Ti_8B_{16} to Mg_8B_{16}, the increase in a is ≈1.3% whereas the increase in c is ≈4.5%. The slight increase in a is also reflected in the variation of the intraplanar distance, R_{B-B}, as expected. The calculated lattice parameters for Mg_8B_{16} are in very good agreement with previously reported experimental[52–56] and theoretical studies.[30,57–60] Note that the values of the bulk modulus and its pressure derivative obtained using the calculated energy surface (i.e., total energy versus volume) numerically fitted to the static equation of state (EOS) are given as supplementary information.[61]

The calculated cohesive energy with respect to atomic constituents comes out to be 10.36 eV for Ti_8B_{16} gradually decreasing to 9.16 eV for Mg_8B_{16}. Considering that only a small change occurs for a, the expansion in c in going from Ti_8B_{16} to Mg_8B_{16} can mainly be attributed to the weaking of

TABLE I. Structural properties of $Mg_xTi_{1-x}B_2$. For TiB_2, the experimental values of a and c are 3.028 and 3.228 Å, respectively.[51] For MgB_2, the experimental values of a and c are 3.086 and 3.521 Å, respectively.[53]

	Ti_8B_{16}	$Mg_1Ti_7B_{16}$	$Mg_2Ti_6B_{16}$	$Mg_4Ti_4B_{16}$	$Mg_6Ti_2B_{16}$	$Mg_7Ti_1B_{16}$	Mg_8B_{16}
Lattice parameters,							
a (Å)	3.0238	3.0192	3.0279	3.0329	3.0457	3.0527	3.0638
c (Å)	3.2254	3.2666	3.2872	3.3312	3.3611	3.3694	3.3720
Volume per unit cell (Å^3)	25.54	25.79	26.10	26.54	27.00	27.19	27.41
Density (gm/cm^3)	4.55	4.31	4.07	3.63	3.20	2.99	2.79
Bond distance [R_{B-B} (Å)]	1.746	1.743	1.748	1.751	1.758	1.757	1.769
Cohesive energy/atom (eV)	10.36	10.18	10.01	9.72	9.43	9.29	9.16
Binding energy/atom (eV)		0.025	0.039	0.037	0.032	0.016	

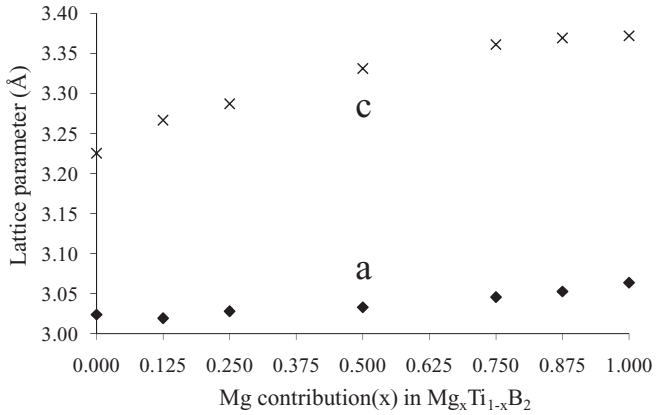

FIG. 2. Lattice parameters a and c vs the amount of Mg in $Mg_xTi_{1-x}B_2$.

the intraplanar bonds along the c direction yielding a lower cohesive energy for Mg_8B_{16} relative to Ti_8B_{16}. Table I also shows the binding energy of the mixed system with respect to its constituent, suggesting $Mg_xTi_{1-x}B_2$ to be stable for all values of x.

Figure 3 shows contours of the projected valance-band charge density for Ti_8B_{16}, $Mg_4Ti_4B_{16}$, and Mg_8B_{16}. The planar YZ cross-sectional projection across the hexagonal axis shows the interaction between the metallic Ti planes in Ti_8B_{16} which appears to decrease when Ti is replaced by Mg in $Mg_4Ti_4B_{16}$. No interaction between Mg planes is seen for Mg_8B_{16}, where the charge-density contours only show

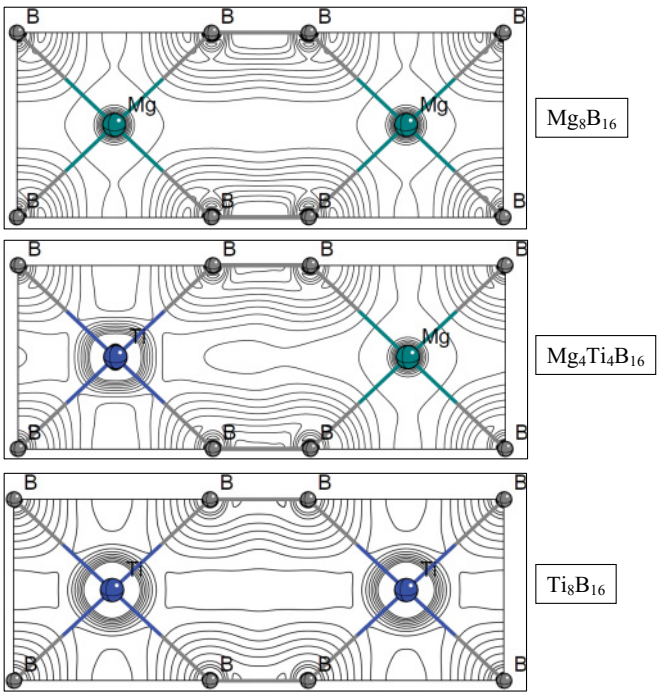

FIG. 3. (Color online) The valance-band charge-density contours for Ti_8B_{16}, $Mg_4Ti_4B_{16}$, and Mg_8B_{16}. The YZ cross-sectional projection across the hexagonal axis shows the Mg and Ti atoms lying above and below the horizontal graphene-type boron layers.

the presence of covalent-type B-B bonding features of the hexagonal boron layers.

The predicted stability of Ti-rich diborides relative to Mg-rich diborides can therefore be understood in terms of the presence of interplanar interactions along the c axis between Ti atoms in the lattice. Furthermore, the calculated total and projected densities of states (not shown here) confirm the presence of dominant Ti bands in Ti-rich diborides. There is also a finite density of states at the Fermi energy, suggesting that the nature of diborides is metallic, as also suggested by their calculated band structures (not shown here). There is a small charge transfer ($\approx 0.2e$) from Ti to B revealed by a Mulliken charge analysis of Ti-rich diborides.

B. Elastic properties

The calculated elastic properties, including elastic constants, bulk and shear moduli, and percentage of anisotropy of $Mg_xTi_{1-x}B_2$, are listed in Table II and illustrated in Fig. 4. Here, B_X is the X-axis elasticity in a system under hydrostatic pressure, K is the bulk modulus, and G is the shear modulus. The percentage of anisotropy[62] of the elastic modulus is defined as $(B_X - B_Z)/B_Z \times 100\%$ and those of K and G are $(K_V - K_R)/(K_V + K_R) \times 100\%$ and $(G_V - G_R)/(G_V + G_R) \times 100\%$. The Voigt estimate is labeled as V and the Reuss estimate is labeled as R. For these calculations, we follow the methodology that is developed in Ref. 63. A^U is the universal anisotropy index.[64] Note that there are six different elastic coefficients—$C_{11}, C_{12}, C_{13}, C_{33}, C_{44}$, and C_{66}—associated with a hexagonal crystal structure such as TiB_2, although C_{66} can be written as $(C_{11} - C_{12})/2$.

The calculated elastic constants $C_{\alpha\beta}$ show a gradual decrease in their values as we go from Ti-rich to Mg-rich diborides. We notice that the $C_{\alpha\beta}$ values of Mg_8B_{16} are about 60%–90% of C_{ij} of Ti_8B_{16}, with the exception of C_{44}. A significant decrease in C_{44} is predicted for Mg-rich diborides relative to Ti-rich borides, thus representing a higher resistance to deformation with respect to a shearing stress in the latter case. The calculated values of elastic (E), bulk (K), and shear (G) moduli of Ti_8B_{16} are in agreement with the previously reported theoretical and experimental studies.

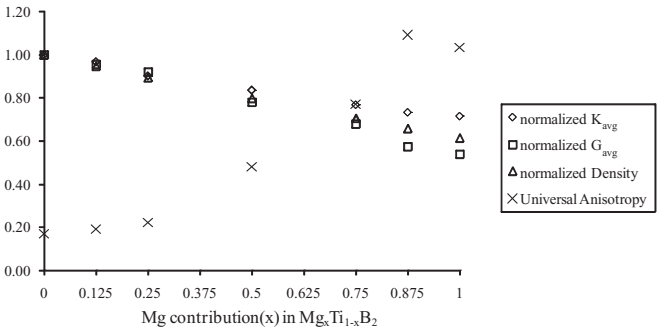

FIG. 4. Average bulk modulus (K_{av}), average shear modulus (G_{av}), density, and universal anisotropy (A^U) vs the amount of Mg in the alloy $Mg_xTi_{1-x}B_2$. The values for the bulk modulus, shear modulus, and density have been normalized by dividing by the corresponding value for TiB_2 for a clearer comparison.

TABLE II. Elastic properties of $Mg_xTi_{1-x}B_2$ at the B3LYP-DFT level of theory. Voigt estimate is labeled as V and Reuss estimate is labeled as R. For polycrystalline TiB_2, the experimental values of E, K, and G are 584.7, 247.5, and 264.3 GPa, respectively.[24]

	Ti_8B_{16}	$Mg_1Ti_7B_{16}$	$Mg_2Ti_6B_{16}$	$Mg_4Ti_4B_{16}$	$Mg_6Ti_2B_{16}$	$Mg_7Ti_1B_{16}$	Mg_8B_{16}
Elasticity tensor							
C_{11} (GPa)	754.6	737.7	714.1	664.0	615.5	562.1	525.7
C_{12} (GPa)	74.4	75.4	64.7	66.4	59.1	56.0	66.3
C_{13} (GPa)	102.9	93.5	71.4	52.8	43.8	64.3	59.2
C_{33} (GPa)	500.9	492.1	480.1	469.7	447.7	403.0	406
C_{44} (GPa)	265.4	240.9	221.1	158.7	124.5	96.8	90.4
C_{66} (GPa)	340.1	331.2	324.7	298.8	278.2	253.0	229.7
Ratio C_{66}/C_{44}	1.3	1.4	1.5	1.9	2.2	2.6	2.5
Elastic modulus							
B_X (GPa)	990	970	890	810	738	711	637
B_Z (GPa)	632	636	572	540	508	492	493
% anisotropy	44	42	44	40	37	36	31
Bulk modulus							
Voigt, K_V (GPa)	286	277	258	238	219	211	203
Reuss, K_R (GPa)	278	269	250	231	214	206	200
K_{av} (GPa)	282	273	254	235	216	209	201
% anisotropy	1.4	1.5	1.6	1.4	1.2	1.0	0.8
Shear modulus							
Voigt, G_V (GPa)	290	276	267	232	208	179	167
Reuss, G_R (GPa)	281	268	257	213	181	148	139
G_{av} (GPa)	285	272	262	222	194	163	153
% anisotropy	1.4	1.6	1.9	4.1	6.8	9.5	9.2
Universal anisotropy, A^U	0.17	0.19	0.22	0.48	0.77	1.07	1.03

For example, the experimental[24] (calculated) values of E, K, and G are 584.7 (632), 247.5 (282), and 264.3 (285) GPa, respectively. It should be noted that due to difficulties in growing high-quality single crystals of TiB_2 or MgB_2, measurements on single crystals of these materials are scarce.[4,17,24] Several experimental investigations were performed, however, on polycrystalline samples of these materials,[2,23] leading to a large scatter of reported values in the scientific literature. Furthermore, experimenters conducting neutron-diffraction measurments at pressures up to 0.62 GPa (Ref. 55) considered MgB_2 to be anisotropic in thermal expansion and compressibility with a disproportionate response along the c axis. Other experiments using x-ray powder diffraction conducted at higher pressures characterized the anisotropic behavior of MgB_2 to be only small over a pressure range up to 8 GPa (Ref. 53) to moderate[54] in bonding behavior between the a and c lattice parameters for pressures up to 6.15 GPa.

The elastic response of a hexagonal crystal such as TiB_2 is expected to show some extent of elastic anisotropy. Considering C_{66}/C_{44} to represent a degree of the shear elastic anisotropy in a hexagonal crystal, we find Ti_8B_{16} to be associated with finding a low shear-mode elastic anisotropy, as also seen experimentally.[24] Interestingly, the shear elastic anisotropy remains nearly the same up to 25% Mg in $Mg_xTi_{1-x}B_2$. It then increases to 2.5 for Mg_8B_{16}, suggesting that it exhibits a strong elastic anisotropy. Note that $C_{66}/C_{44} = 1$ represents the case of elastic isotropy.

Recently, Ranganathan and Ostoja-Starzewski introduced a universal elastic anisotropy index A^U whose nonzero value expresses the extent of single-crystal anisotropy accounting for both the shear and the bulk contributions.[64] The calculated A^U is small for Ti-rich borides, becoming large for Mg-rich diborides. It is 1.03 for Mg_8B_{16}, indicating its large elastic anisotropy.

IV. CONCLUSIONS

In summary, we find that the elastic properties of $Mg_xTi_{1-x}B_2$ ($0 \leqslant x \leqslant 1$) can be grouped into two categories: a small elastic anisotropy with relatively large bulk and shear moduli is predicted for Ti-rich diborides with $x < 0.25$, whereas Mg-rich diborides are predicted to be associated with a large elastic anisotropy and relatively small bulk and shear moduli. The predicted elastic behavior is confirmed by the nature of chemical bonding in $Mg_xTi_{1-x}B_2$; there is a noticeable participation of interplanar metal-metal bonds in Ti-rich diborides, whereas the intraplanar B-B bonds dominate in Mg-rich diborides. The interplanar bonds in Ti-rich diborides keep boron layers from moving with respect to each other, whereas boron layers shift easily in the absence of the interplanar bonds in Mg-rich diborides, leading to a relatively large anisotropy in the shear modulus.

The calculated results, therefore, provide a guideline to design a lower-density yet isotropically hard $Mg_xTi_{1-x}B_2$

alloy. Upon doping of Mg atoms into the lattice ($x \leqslant 0.25$), the density of the material is decreased with only a marginal decrease in elastic moduli and a slight increase in elastic anisotropy. An $Mg_xTi_{1-x}B_2$ material with elastic properties comparable to TiB_2 yet lower in density is predicted. When $x > 0.25$, however, the paucity of Ti-Ti interplanar bonds is manifested in $Mg_xTi_{1-x}B_2$ materials that exhibit more shearing behavior along boron layers. Although much less dense, these materials become highly anisotopic in their elastic behavior and would be much less favored as replacements for TiB_2 in technological applications.

ACKNOWLEDGMENTS

Helpful discussions with Manuel Recio are acknowledged. This work was partially supported by the RDECOM-ARL: Army Research Laboratory through Contracts No. W911NF-07-D-0001 and No. W911NF-09-2-0026.

*pandey@mtu.edu
†datta.dandekar@us.army.mil

[1] J. Hoard and R. Huges, *Chemistry of Boron and Its Compounds* (Wiley, New York, 1967).
[2] R. Munro, J. Res. Natl. Inst. Stand. Technol. **105**, 709 (2000).
[3] J. Castaing and P. Costa, in *Boron and Refractory Borides*, edited by V. I. Matkovich (Springer-Verlag, New York, 1977), p. 390.
[4] J. J. Gilman and B. W. Roberts, J. Appl. Phys. **32**, 1405 (1961).
[5] D. E. Wiley, W. R. Manning, and O. Hunter, J. Less-Common Met. **18**, 149 (1969).
[6] W. H. Gust, A. C. Holt, and E. B. Royce, J. Appl. Phys. **44**, 550 (1973).
[7] *LASL Shock Hugoniot Data*, edited by S. P. March (University of California Press, Berkeley, CA, 1980).
[8] M. K. Ferber, P. F. Becher, and C. B. Finch, J. Am. Ceram. Soc. **66,** C-2 (1983).
[9] V. J. Tennery, C. B. Finch, C. S. Yust, and G. W. Clark, in *Science of Hard Materials*, edited by R. K. Viswanadham (Plenum, New York, 1983), p. 891.
[10] H. R. Baumgartner and R. A. Steiger, J. Am. Ceram. Soc. **67**, 207 (1984).
[11] P. F. Becher, C. B. Finch, and M. K. Ferber, J. Mater. Sci. Lett. **5**, 195 (1986).
[12] R. A. Andrievski and B. U. Asanov, J. Mater. Sci. Lett. **10**, 147 (1991).
[13] A. Abbate, J. Frankel, and D. P. Dandekar, in *Recent Trends in High Pressure Research*, edited by A. K. Singh (Oxford, New Delhi, 1992), p. 881.
[14] A. Bellosi, T. Graziani, S. Guicciardi, and A. Tampieri, *Special Ceramics 9, British Ceramic Proceedings No. 49* (Institute of Ceramics, Stoke on Trent, 1992), p. 163.
[15] D. P. Dandekar and D. C. Benefanti, J. Appl. Phys. **73**, 673 (1993).
[16] S. I. Wright, J. Appl. Crystallogr. **27**, 794 (1994).
[17] P. S. Spoor, J. D. Maynard, M. J. Pan, D. J. Green, J. R. Hellmann, and T. Tanaka, Appl. Phys. Lett. **70**, 1959 (1997).
[18] S. P. Dodd, M. Cankurtaran, G. A. Saunders, and B. James, J. Mater. Sci. **36**, 3989 (2001)
[19] D. P. Dandekar and E. J. Rapacki, *Ceramic Transactions* (American Ceramic Society, Westerville, Ohio, 2002), vol. 134.
[20] G. M. Amulele and M. H. Manghnani, J. Appl. Phys. **97**, 023506 (2005).
[21] G. M. Amulele, M. H. Manghnani, and M. Somayazulu, J. Appl. Phys. **99**, 023522 (2006).
[22] I. R. Shein and A. L. Ivanovskii, J. Phys. Condens. Matter **20**, 415218 (2008).
[23] D. P. Dandekar, Mater. Sci. Forum **638–642**, 1023 (2010)
[24] H. Ledbetter, J. Res. Natl. Inst. Stand. Technol. **114**, 333 (2009).
[25] D. C. Tian and X. B. Wang, J. Phys. Condens. Matter **4**, 8765 (1992).
[26] P. E. van Camp and V. E. van Doren, High Press. Res. **13**, 335 (1995).
[27] K. Lie, R. Brydson, and H. Davock, Phys. Rev. B **59**, 5361 (1999).
[28] C. A. Perottoni, A. S. Pereira, and J. A. H. da Jornada, J. Phys. Condens. Matter **12**, 7205 (2000).
[29] P. Vajeeston, P. Ravindran, C. Ravi, and R. Asokamani, Phys. Rev. B **63**, 045115 (2001).
[30] V. Milman and M. C. Warren, J. Phys. Condens. Matter **13**, 5585 (2001).
[31] K. B. Panda and K. S. Ravi Chandran, Comput. Mater. Sci. **35**, 134 (2006).
[32] F. Penga, H.-Z. Fua, and X.-L. Cheng, Physica B **83**, 400 (2007).
[33] I. R. Shein and A. L. Ivanovskii, J. Phys. Condens. Matter **20**, 425218 (2008).
[34] C.-L. Wang, B.-H. Yu, and H.-L. Huo, Chin. Phys. B **18**, 1248 (2009).
[35] Y. Zhao, Y. Feng, C. H. Cheng, L. Zhou, Y. Wu, T. Machi, Y. Fudamoto, N. Koshizuka, and M. Murakami, Appl. Phys. Lett. **79**, 1154 (2001).
[36] Y. Zhao, Y. Feng, C. H. Cheng, T. Machi, N. Koshizuka, and M. Murakami, Appl. Phys. Lett. **80**, 1640 (2002).
[37] S. Haigh, P. Kovac, T. A. Prikhna, Y. M. Savchuk, M. R. Kilburn, C. Salter, J. Hutchison, and C. Grovenor, Supercond. Sci. Technol. **18**, 1190 (2005).
[38] R. Dovesi, R. Orlando, B. Civalleri, R. Roetti, V. R. Saunders, and C. M. Zicovich-Wilson, Z. Kristallogr. **220**, 571 (2005); R. Dovesi, V. R. Saunders, R. Roetti, R. Orlando, C. M. Zicovich-Wilson, F. Pascale, B. Civalleri, K. Doll, N. M. Harrison, I. J. Bush, P. D'Arco, and M. Llunell, *CRYSTAL09 User's Manual* (University of Torino, Torino, 2009).
[39] A. D. Becke, Phys. Rev. A **38**, 3098 (1988).
[40] C. Lee, W. Yang, and R. G. Parr, Phys. Rev. B **37**, 785 (1988).
[41] R. Pandey, M. Causa, N. Harrison, and M. Seel, J. Phys. Condens. Matter **8**, 1 (1996).
[42] R. Pandey, P. Zapol, and M. Causa, Phys. Rev. B **55**, R16009 (1997).
[43] R. Pandey, M. Rérat, C. Darrigan, and M. Causa, J. Appl. Phys. **88**, 6462 (2000).
[44] H. Jiang, R. Orlando, M. A. Blanco, and R. Pandey, J. Phys. Condens. Matter **16**, 3081 (2004).
[45] H. He, R. Orlando, M. A. Blanco, R. Pandey, E. Amzallag, I. Baraille, and M. Rérat, Phys. Rev. B **74**, 195123 (2006).

[46]K. C. Lau, R. Orlando, and R. Pandey, J. Phys. Condens. Matter **21**, 045304 (2009).
[47]D. Groh, R. Pandey, M. Sahariah, E. Amzallag, I. Baraille, and M. Rérat, J. Phys. Chem. Solids **70**, 789 (2009).
[48]All details regarding the basis sets employed in the calculations discussed in this study can be obtained from the authors (pandey@mtu.edu).
[49]See supplemental material at [http://link.aps.org/supplemental/10.1103/PhysRevB.83.115122] for the dependence of structural properties of $Mg_4Ti_4B_{16}$ on the boron basis set.
[50]W. F. Perger, J. Criswell, B. Civalleri, and R. Dovesi, Comp. Phys. Comm. **180**, 1753 (2009).
[51]A. H. Silver and T. Kushida, J. Chem. Phys. **38**, 865 (1963).
[52]M. E. Jones and R. E. Marsh, J. Am. Chem. Soc. **76**, 1434 (1954).
[53]T. Vogt, G. Schneider, J. A. Hriljac, G. Yang, and J. S. Abell, Phys. Rev. B **63**, 220505 (2001).
[54]K. Prassides *et al*., Phys. Rev. B **64**, 012509 (2001).
[55]J. D. Jorgensen, D. G. Hinks, and S. Short, Phys. Rev. B **63**, 224522 (2001).
[56]A. F. Goncharov, V. V. Struzhkin, E. Gregoryanz, J. Hu, R. J. Hemley, H.-K. Mao, G. Lapertot, S. L. Bud'ko, and P. C. Canfield, Phys. Rev. B **64**, 100509(R) (2001).
[57]P. Ravindran, P. Vajeeston, R. Vidya, A. Kjekshus, and H. Fjellvag, Phys. Rev. B **64**, 224509 (2001).
[58]A. K. M. A. Islam and F. N. Islam, Physica C **363**, 189 (2001).
[59]I. Loa and K. Syassen, Solid State Commun. **118**, 279 (2001).
[60]H.-Z. Guo, X.-R. Chen, J. Zhu, L.-C. Cai, and J. Gao, Chin. Phys. Lett. **22**, 1764 (2005).
[61]See supplemental material at [http://link.aps.org/supplemental/10.1103/PhysRevB.83.115122] for the values of the bulk modulus and its pressure derivative obtained using the calculated energy surface (i.e., total energy versus volume) numerically fitted to the static equation of state (EOS).
[62]D. H. Chung and W. R. Buessem, *Anisotropy in Single-Crystal Refractory Compounds*, edited by F. W. Vahldiek and S. A. Mersol (Plenum, New York, 1968), Vol. 2, p. 217.
[63]S. Cowin, Q. J. Mech. Appl. Math. **42**, 249 (1989).
[64]S. I. Ranganathan and M. Ostoja-Starzewski, Phys. Rev. Lett. **101**, 055504 (2008).